Remote-sensing observations of coastal sub-mesoscale eddies in the south-eastern Baltic

Evgenia Gurova[*]
Boris Chubarenko

Atlantic Branch of the P. P. Shirshov Institute of Oceanology
of the Russian Academy of Sciences (IO RAS),
Pr. Mira 1, 236000 Kaliningrad, Russia;

e-mail: evguruna@gmail.com

[*]corresponding author

Abstract

This paper presents an overview of the sub-mesoscale eddies observed in the coastal zone of the south-eastern Baltic near the shores of the Sambian Peninsula and the Curonian Spit based on CODAR (high-frequency coast-based radar) measurements and analysis of MODIS and ASAR satellite images for the period 30 March 2000–31 December 2011. It was found that when winds are predominantly SW, S or W, a wake eddy of varying size (up to 25 km in diameter) forms off Cape Taran and can cover the area between the shoreline and the 65 m isobath. Its longest lifetime, observed using MODIS images, was 6 days. Another location where coastal sub-mesoscale eddies (up to 10–15 km in diameter) of varying form regularly appear is the coastal slope near the southern and central part of the Curonian Spit.

1. Introduction

Mesoscale eddies appear over the continental slope at the edge of the main deep water basin circulation due to the baroclinic instability of the

The complete text of the paper is available at http://www.iopan.gda.pl/oceanologia/

main current. Diameters of such eddies are between 2 and 7 of R_d, where R_d is the local Rossby radius of baroclinic deformation (Zatsepin et al. 2011). At the next level of the cascade of energy dissipation are the smaller sub-mesoscale eddies (radius $< R_d$). These are of the scales of 1–10 km and 1–100 hours and are formed over the shelf and coastal slope, and their evolution depends very much on bottom topography and coastal orography (Zatsepin et al. 2011). Flow disturbance caused by coastal obstacles (or an island) leads to the generation of a wake eddy located on the lee side (Chubarenko et al. 2000, Harlan et al. 2002). All these eddy structures play an important role in horizontal and vertical mixing, contributing significantly to coastal – open sea water exchange (Bassin et al. 2005), and also having an influence on coastal morpho- and lithodynamic processes.

The study area (Figure 1), the south-eastern Baltic (SEB), is characterized by relatively high rates of erosion, the range of mean rates being 0.2–1.5 m per year for the whole coastline, depending on the period of calculation (Chubarenko et al. 2009). Wave impact, regular occurrences of vortex circulation cells, rip currents and longshore currents all exist due to the heterogeneity of the coastline and bottom topography, and they are usually identified as the causes of erosion (Ryabkova 1987, Boldyrev et al. 1992, Zhindarev et al. 1998, Babakov 2003, 2010). The first direct observations of a coastal eddy, near the base of the Curonian Spit, were made using the high frequency CODAR system in 2006 (Gorbatskiy et al. 2007).
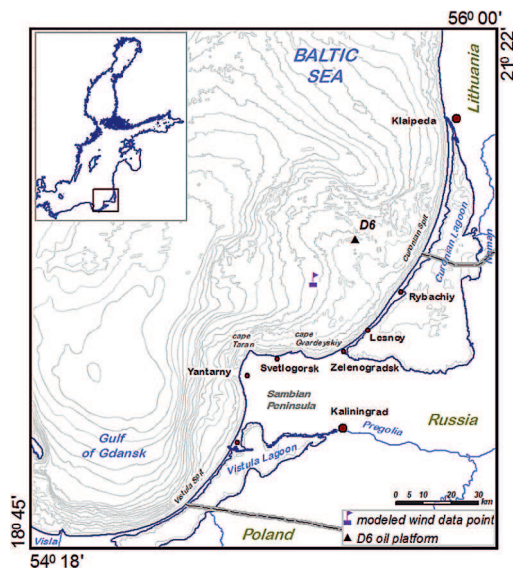

Figure 1. Overview map of the research area with the locations of oil-field platform D6 and BSIOM grid point for the modelled wind data

In contrast to in situ measurements, which are rather consuming in terms of financial and human resources, and therefore limited in regularity, space and time, remote sensing techniques – optical, thermal and radar – offer a more flexible approach to investigating the structure and elements of coastal currents (Karabashev et al. 2005, Gurova 2009).

Conditions in SEB are highly favourable for the visualization of current structures in remotely-sensed observations. Erosion of sandy coasts and bottom sediments increases the turbidity of coastal waters (Emelyanov 1968, Emelyanov (ed.) 2001); large rivers (the Vistula, Neman and Pregolia) bring suspended sediments and coloured dissolved organic material (CDOM); in addition, algae and cyanobacteria blooms accumulate at the water surface and in the upper layers and influence the optical properties of the water (IOCCG 2000, Aneer & Löfgren 2007, Gurova & Ivanov 2011).

All these factors change the water colour non-uniformly along the coastline and at different parts of the optical spectrum. Knowledge of the local sources of colouring agents enables analysis of the longshore water exchange. Temperature is one of the main hydrological parameters describing the water properties and water mass boundaries. Synthetic aperture radar (SAR) data can image the water's dynamic features from the heterogeneity of sea surface roughness. This heterogeneity is due to the presence of micro-capillary waves, biogenic and chemical slicks, as well as other objects and substances at the water surface (Johannessen et al. 1994, Ivanov & Ginzburg 2002, Ivanov 2010). Combined use of different types of passive and active remote sensing data provides even more opportunities for detailed analysis of marine processes.

In this paper we present some evidence of the existence of sub-mesoscale eddies in SEB. Using the results of remote observations by the CODAR system as well as satellite images, we identified sub-mesoscale eddies within an 11-year archive of different types of remote sensing data, grouping the cases observed by typical geographical location, and analysing the spatial, temporal, spectral and meteorological characteristics.

2. Data and methods

Firstly, the low resolution satellite images which exhibited coastal eddies were selected from the 11-year (30 March 2000–31 December 2011) archive of the MODIS (Terra and Aqua) open-access Level 1 and Atmosphere Archive and Distribution System (LAADS) by NASA[1]. For an overview of the situation, the images were pre-processed by CREFL_SPA algorithm (by

---

[1]http://ladsweb.nascom.nasa.gov/data/

NASA DRL)[2] of atmospheric correction, and then 'land' bands 1 (250 m spatial resolution), 3 and 4 (500 m spatial resolution), were merged into an RGB (1-4-3) composite with resolution 250 m pixel^{-1}. The higher spatial resolution (250–500 m) and bigger spectral width (20 nm) of MODIS visual 'land' bands are very informative for the visual identification and analysis of turbid coastal water features compared to the spectrally narrow (10 nm) and spatially less detailed (1 km) MODIS 'ocean' bands (Gurova 2009). However, for the spectral analysis of these features we used normalized water leaving radiances (nLw) (Gordon & Wang 1994) and spectral diffuse attenuation coefficients of downwelling irradiance Kd_Lee (Lee et al. 2005), calculated from the 'ocean' bands (8–16), specially designed for such purposes. Images were processed from L1A level with Seadas 6.2[3] software, using the MUMM atmospheric correction algorithm (Ruddick et al. 2000), which is the best suited to turbid Baltic Sea waters (Woźniak et al. 2008). CDOM absorption coefficients $a_{CDOM}(400)$ were calculated using an empirical algorithm specially developed for the Baltic Sea and successfully validated (Kowalczuk et al. 2005, 2010). MODIS Sea Surface Temperature (SST) products were calculated with the standard algorithm implemented in Seadas 6.2 (Brown & Minnett 1999).

Wide Swath Mode images from Advanced Synthetic Aperture Radar (ASAR instrument on board the Envisat satellite) were obtained from ESA archives. With a medium spatial resolution of 75 m pixel^{-1}, the ASAR WSM images, especially those obtained by multi-sensor approach, are very useful for detailed spatial analysis of hydrodynamic features affecting the water surface (Gurova & Ivanov 2011).

Secondly, examples of submesoscale eddies in SEB were selected from a series of measurements of sea surface currents in the marine area near the Curonian Spit (the Zelenogradsk-Rybachiy section) and the northern shore of the Sambian Peninsula, made by the coastal radar Sea Sonde CODAR system in 2006 and 2007. Two resolutions for a 30×30-cell grid were used in these measurements – 500 m cell^{-1} and 250 m cell^{-1} (Gorbatsky et al. 2007, Babakov et al. 2008).

To analyse the wind statistics we used wind data at altitude 10 m from a coupled sea-ice-ocean model of the Baltic Sea (BSIOM) with a spatial resolution of 1.2 nautical miles, which has been shown to provide realistic values when compared to field measurements (Rudolph & Lehmann 2006). Verification comparison of modelling data for a 6-hour average wind with measurements at point D6, located 20 km from the coast of the Curonian

---

[2]http://directreadout.sci.gsfc.nasa.gov/?id=software
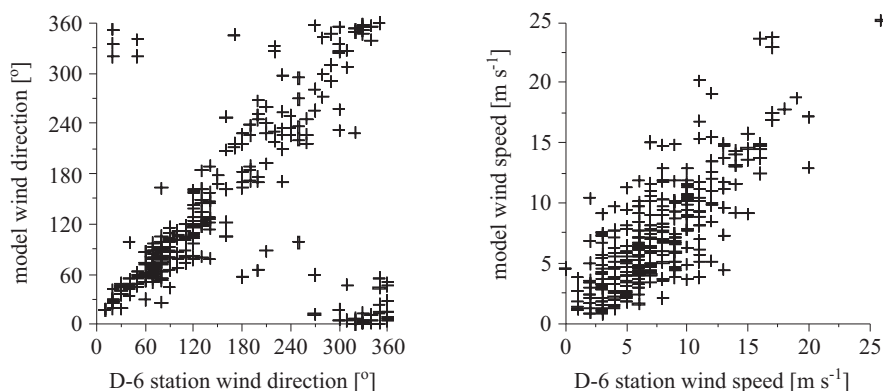[3]http://oceancolor.gsfc.nasa.gov/seadas/

Figure 2. Comparison of 6-hour average wind data at the BSIOM model grid point (modelled) and weather station D-6 (measured), located near the Curonian Spit (Figure 1) for a period of 92 days

Spit, for a period of 92 days, showed general correspondence between the modelled data and measurements (Figure 2). Therefore, the wind statistics in this paper (Table 1 (see page 639) and wind diagrams in Figure 7 (see page 644)) were obtained using BSIOM data.

3. Results and discussion

The most representative examples of various coastal sub-mesoscale eddies measured by CODAR and identified on satellite images in the area of research are presented in Figures 3–5. These illustrate a relatively fixed location of the structures along the coastline, namely in the following areas: the northern and western coast of the Sambian Peninsula (to the east and to the west of Cape Taran respectively), and the base and central sections of the Curonian Spit. In each of these places eddy structures have their specific hydrological, optical and spatial properties, which have been analysed using multiple MODIS satellite images, additionally by SAR images for detailed surface structure analysis, and also CODAR field measurements. Information about the observed sub-mesoscale eddies are presented, together with corresponding wind data, in Tables 1 and 2. Below we will describe each group of eddies according to their location.

3.1. Northern shore of the Sambian Peninsula

The sub-mesoscale eddy near the northern shore of the Sambian Peninsula (hereafter referred to as the N-Sambian eddy) was identified, at different stages of development, in approximately 400 MODIS images over the 11-year period (30 March 2000–31 December 2011). In this paper only
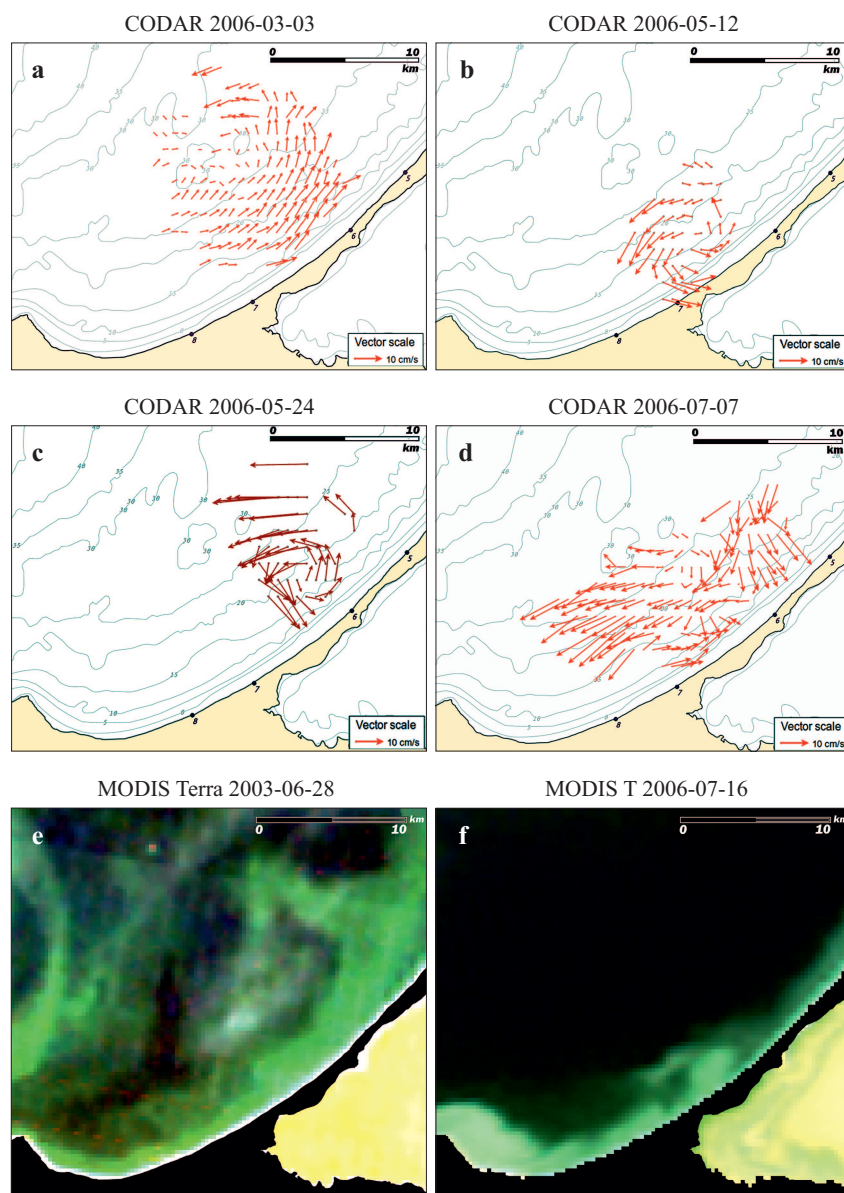
CODAR 2006-03-03

CODAR 2006-05-12

CODAR 2006-05-24

CODAR 2006-07-07

MODIS Terra 2003-06-28

MODIS T 2006-07-16

Figure 3. Coastal eddies, measured by CODAR (a–d) and detected on 250 m RGB-143 MODIS (A – Aqua, T – Terra) images (e, f)

the most evident and well-developed cases are analysed (see the examples in Figures 4c–f, 5a–b). This vortex is always adjacent both to Cape Taran, located along the shore section between Cape Taran and the next cape eastwards (Cape Gvardeyskiy), and has an anticyclonic circulation. The diameter of this vortex varies from 8–10 km to 20 km (Figure 6).

MODIS T 2003-09-06

MODIS T 2003-04-01

CODAR 2006-09-13 and MODIS A 2004-04-13

MODIS T 2000-04-17

MODIS Aqua 2003-06-17

MODIS Aqua 2010-07-03
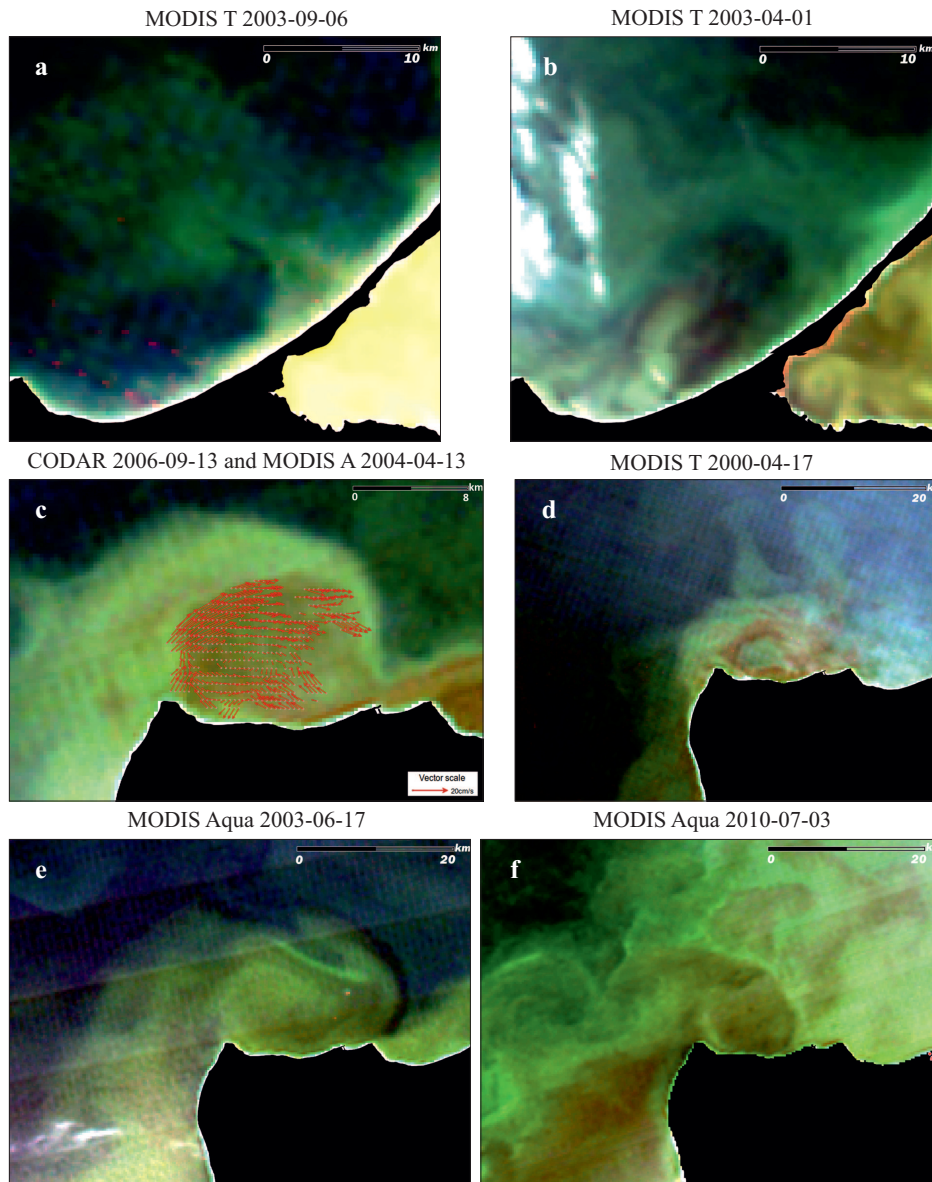
Figure 4. Coastal eddies, identified on 250 m RGB-143 MODIS images (A – Aqua, T – Terra) and measured by CODAR, which fit each other well (c)

The histogram of the N-Sambian eddy's distribution of diameters, based on 20 cases, is presented in Figure 6, and the individual values are presented in Table 1.

Analysis of the wind during the preceding 48 hours suggests S, SW or variable winds (without the eastern sector prevailing) < 10 m s^{-1}

ASAR 2009-07-17

MODIS A 2009-07-17

MODIS A 2009-08-08

MODIS T 2010-08-16

MODIS A 2005-07-13   MODIS A 2005-01-27   MODIS A 2002-09-02
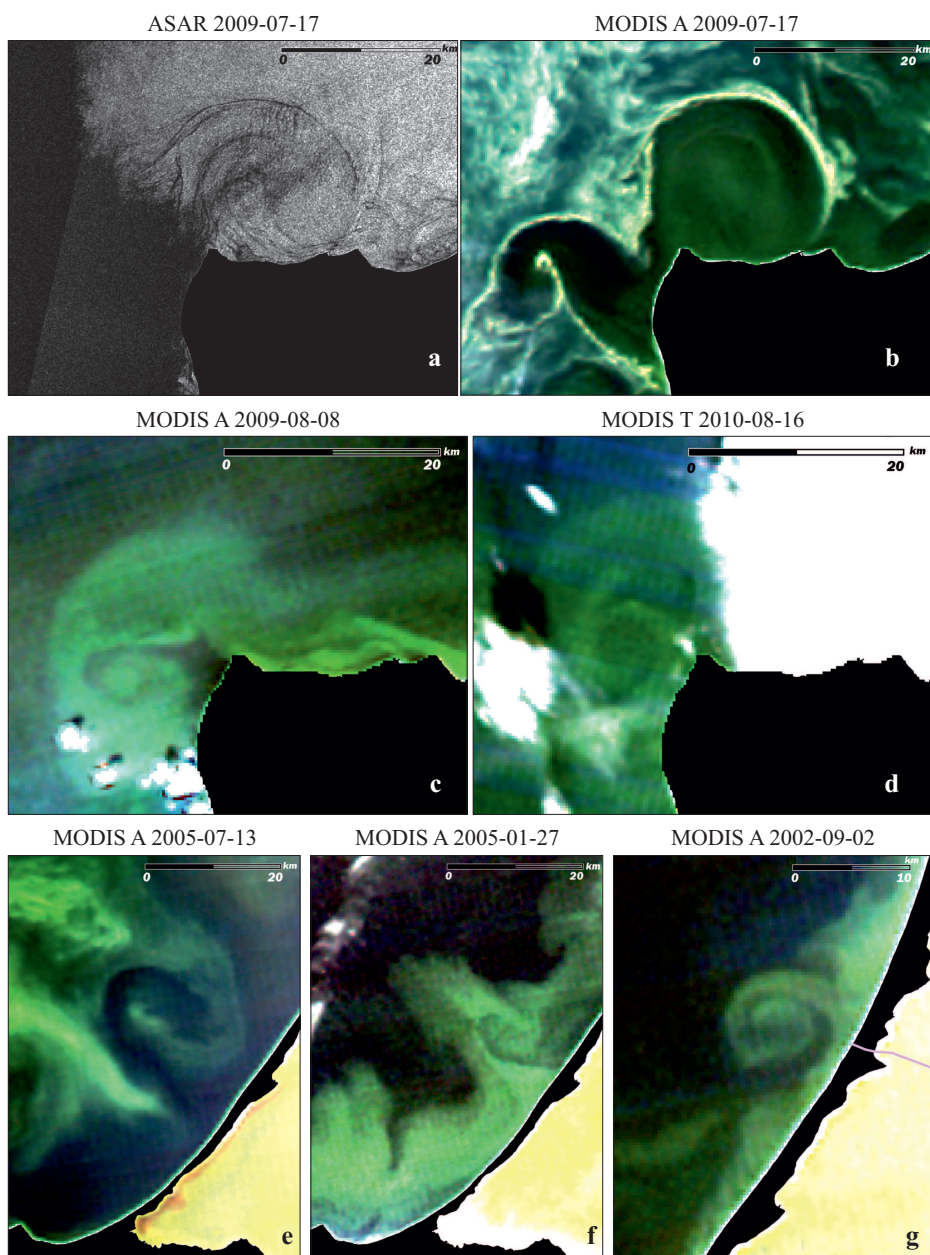
Figure 5. Coastal eddies, identified on ASAR WSM image (a) and on 250 m RGB-143 MODIS (A – Aqua, T – Terra) images (b–g)

as being favourable for eddy formation in this area (Table 1). The histogram of wind speed distribution (Figure 7) demonstrates the predominance of winds < 10–12 m s^{-1}. The wind roses in Figure 7 show

Table 1. Spatial characteristics and wind conditions of observed sub-mesoscale eddies

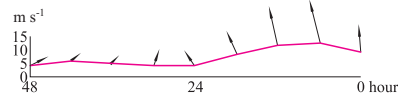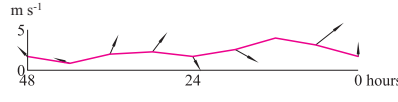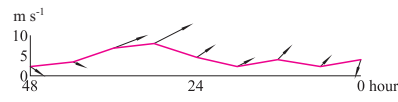| Date	Source	Wind_0 $[\text{m s}^{-1}]^{(1)}$	Wind_{sp} $48^{(2)}$	$\text{D}^{(3)}$	Wind diagram[4]
Sambian Peninsula Northern coast – N-Sambian eddy (*all – anti-cyclonic direction*)					
13.09.2006	CODAR	SE, 4	3–6	10	
17.04.2000	MODIS	SE, 5	2–9	12	
30.04.2002	MODIS	SW, 3	3–9	10	
17.06.2003	MODIS	N, 6	2–6	16	
01.08.2003	MODIS	NE, 3	1–5	10	
04.08.2003	MODIS	NW, 6	1–6	9	
31.03.2004	MODIS	NE, 4	1–5	10	
12.04.2004	MODIS	N, 4	3–7	10	
13.04.2004	MODIS	NE, 2	0–7	13	
14.04.2004	MODIS	SW, 3	0–4	14	
26.05.2005	MODIS	SW, 3	3–10	8	

Table 1. (*continued*)
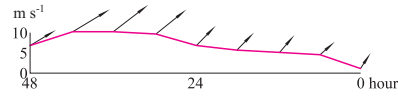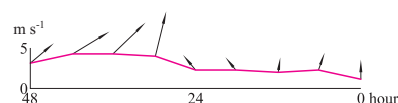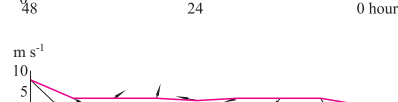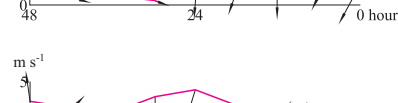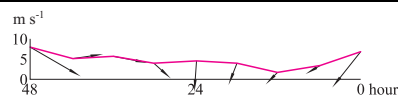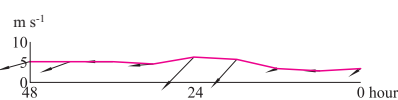
Date	Source	Wind_0 $[\text{m s}^{-1}]^{(1)}$	Wind_{sp} $48^{(2)}$	$D^{(3)}$	Wind diagram[4]
19.07.2005	MODIS	SW, 1	1–10	12	
29.03.2008	MODIS	S, 9	4–12	12	
27.04.2008	MODIS	S, 2	1–4	18	
23.07.2008	MODIS	N, 4	2–8	17	
13.07.2009	MODIS	S, 1	1–4	20	
17.07.2009	MODIS, ASAR	E, 3	2–5	20	
28.05.2010	MODIS	NW, 2	2–8	19	
03.07.2010	MODIS	NE, 5	1–5	12	
15.07.2010	ASAR	SW, 0.4	0–4	20	

Sambian Peninsula Western coast – W-Sambian eddy *(all-cyclonic direction)*

Date	Source	Wind_0	Wind_{sp}	D	Wind diagram
13.07.2002	MODIS	NE, 7	2–8	15	
08.08.2002	MODIS	NE, 3	3–6	11	
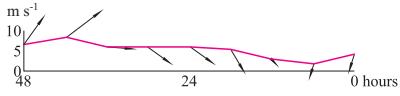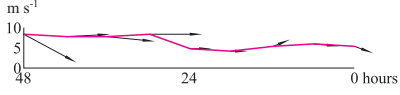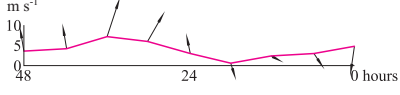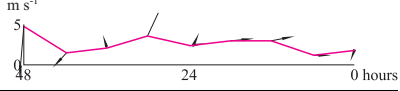
Table 1. (*continued*)

Date	Source	Wind$_0$ [m s^{-1}][1]	Wind$_{sp}$ 48[2]	D[3]	Wind diagram[4]
08.08.2009	MODIS	NE, 4	3–7	22	
16.08.2009	MODIS	SE, 3	1–5	22	

Curonian Spit, root part – Lesnoy eddy *(all-cyclonic direction)*

Date	Source	Wind$_0$	Wind$_{sp}$ 48	D	Wind diagram
03.03.2006	CODAR	SW, 10	2–10	14	
04.04.2006	CODAR	S, 5	5–11	10	
12.05.2006	CODAR	W, 6	3–7	7	
24.05.2006	CODAR	SW, 9	8–12	8.5	
07.07.2006	CODAR	S, 4	2–5	6	
01.04.2003	MODIS	S, 6	3–15	12	
28.06.2003	MODIS	E, 6	4–8	14	
28.05.2005	MODIS	E, 1	1–12	6	
16.07.2006	MODIS	N, 11	8–15	5	

Table 1. (*continued*)

Date	Source	Wind_0 $[\text{m s}^{-1}]^{(1)}$	Wind_{sp} $48^{(2)}$	$D^{(3)}$	Wind diagram$^{(4)}$
28.03.2008	MODIS	SE, 4	4–8	7	
20.05.2008	MODIS	NE, 4	0–5	6	
05.06.2008	MODIS	NE, 6	3–10	4	
04.06.2010	MODIS	N, 13	5–13	4	

Curonian Spit, central part – *anti-cyclonic direction*

Date	Source	Wind_0	Wind_{sp}	D	Wind diagram
26.08.2006	CODAR	SE, 1	1–9	30	
27.01.2005	MODIS	E, 2	1–4	10	
13.07.2005	MODIS	NW, 4	1–6	27	
13.07.2009	MODIS	S, 1	1–4	12	
17.07.2009	MODIS	E, 3	2–5	16	
30.03.2010	MODIS	E, 5	1–9	13	

Table 1. (*continued*)

Date	Source	Wind_0 $[\text{m s}^{-1}]^{(1)}$	Wind_{sp} $48^{(2)}$	$\text{D}^{(3)}$	Wind diagram[4]
02.09.2002	MODIS	N, 4	2–8	10	
22.05.2004	MODIS	W, 5	4–8	8	
09.07.2006	MODIS	N, 5	1–7	20	
11.07.2006	MODIS	NE, 2	1–5	26	

[1] Wind direction and speed during the measurements/observations.
[2] Wind velocity range during the 48 hours before measurement/observation.
[3] Diameter of the sub-mesoscale eddy in km, measured perpendicularly off the coastline.
[4] Wind direction and velocity diagram for 48 hours before measurement/observation.
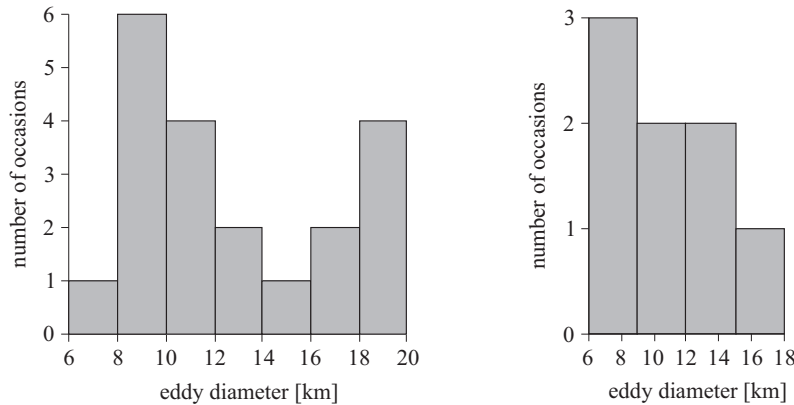
Figure 6. Distribution of diameters for the N-Sambian eddy (left) and the Lesnoy eddy (right)

that low winds < 5 m s^{-1} are variable without any sector prevalence, but when they are < 10 m s^{-1} there is a significant dominance of W-SW winds. Moderate 5–10 m s^{-1} winds are more important for the formation of sea currents. Given this, the formation of the N-Sambian eddy can be assumed to be a regular event, occurring more often than
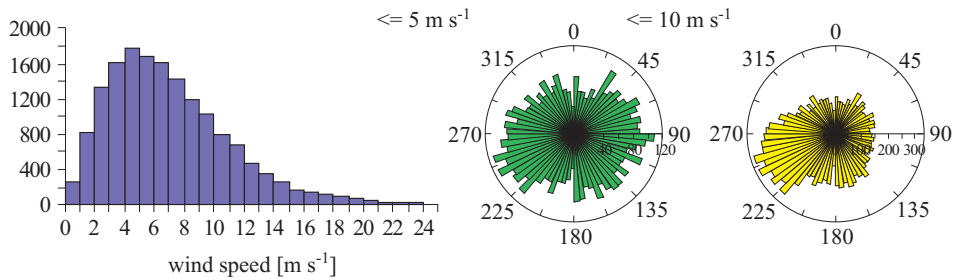
Figure 7. Histogram of wind speed distribution and wind roses at selected points (Figure 1) for the period 1999–2010

can be observed by optical satellite images, the continuity of which is restricted because of the cloudiness in the region.

The maximum lifetime of the eddy in this area, determined by MODIS data, was 6 days (11–16 April 2004), and there were multiple series of 2–3 days.

A detailed surface current measurement of this eddy by CODAR with a 250 m grid resolution was performed in September 2006 and the results fit the form of the eddy perfectly, as observed on another day (Figure 4c). However, on the day of this CODAR measurement, MODIS determined no SST anomaly and only a slight spectral anomaly in this area. This could be further evidence of the existence of this eddy even when it is not visible on optical images. The reason for this could be, for example, the lack of coloured substances in the water at that time. This measurement was made during rather quiet wind conditions (up to 3 m s^{-1}) with the sea state being smooth and mean current speeds were measured at ca 10 m s^{-1}, the range being 0–22 cm s^{-1} (Table 2, see page 649).

In all observed cases the N-Sambian eddy has a quite clear ecliptic or almost perfectly round (Figures 5a–b) enclosed circulation area, its western side always being bounded by Cape Taran. Optical images show that the area within the eddy is frequently homogeneous, so long as the eddy is relatively small. However, if the eddy is well-developed and large it has a heterogeneous internal structure, which may be spiral in form, or which may be alternating closed rings, each with different spectral properties.

The eddy observations dated 17 July 2009 merit detailed examination (Figures 5a–b). At the time of the intensive cyanobacteria bloom, when the sea surface was covered with floating organisms, the well-developed area of the eddy was free from them; however, it was surrounded by a dense borderline with a high accumulation of cyanobacteria. The SAR image of that day shows the spiral structure of the vortex, with a wide stream from the entire coastal boundary of the eddy to its centre. Such a fact should

be considered in any coastal dynamics investigations of this highly eroded area.

Spectral analysis of the N-Sambian eddy shows higher nLw values within the eddy area compared to the waters beyond it in the majority of cases (from the 11 images analysed on Figure 8) and across most of the spectrum, the exception being the blue zone (412, 443 nm) (Figure 8).
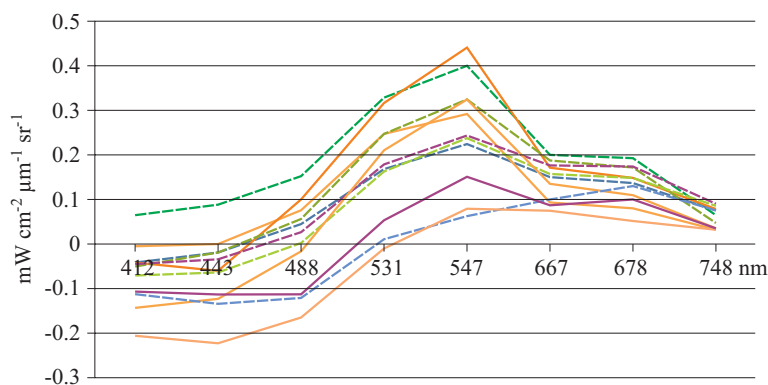
Figure 8. Spectral difference by wavelength between points inside and outside the N-Sambian eddy (calculated as the inside value minus the outside one)

Brightness is maximum along the border area of the eddy, but decreases slightly towards its centre. The profile shown in Figure 9 also illustrates the lowering of nLw_412 values inside the eddy area compared to the surrounding waters, and as well as a significant increase of $a_{CDOM}(400)$ there. As the River Vistula is the nearest significant source of CDOM, a strong absorber of shortwave light (Kowalczuk 1999, Kowalczuk et al. 2005, Woźniak & Dera 2007), this can testify that longshore currents in the Gulf of Gdańsk may

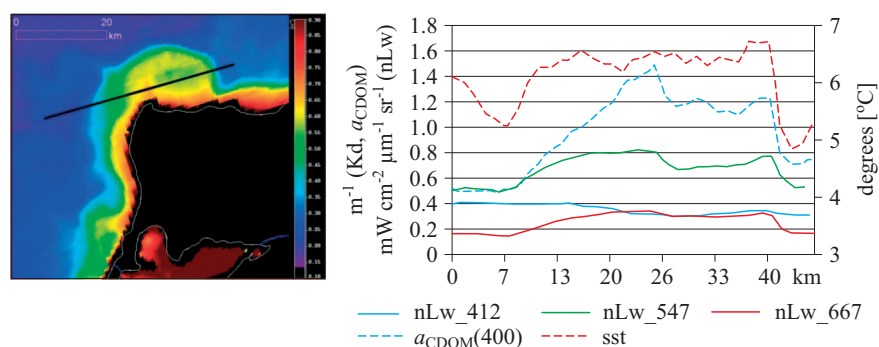**Figure 9.** Kd_488_Lee value distribution with profile line (left) and profile values for nLw 412, 547, 667, SST and $a_{CDOM}(400)$ (right) for 13.04.2004
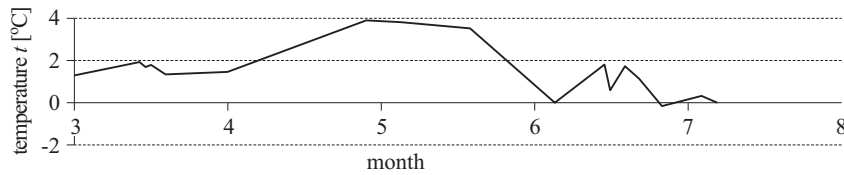
Figure 10. SST difference between points inside and outside the N-Sambian eddy averaged through cases observed each calendar month during the period from 17 April 2000 to 3 July 2010

bring water from the Vistula mouth area (located in the south-west of the study area, see Figure 1) northwards towards Cape Taran on the Sambian Peninsula (Figure 10), and this water then becomes incorporated into the N-Sambian eddy circulation. This is especially important in spring with increasing runoff from the Vistula – the largest river in the region. The influence of the outflow from the Vistula Lagoon (Baltiyskiy Strait), which is geographically closer than the Vistula mouth, is spectrally less significant: the waters flowing in from the Pregolia and other small rivers pass through the Vistula Lagoon, a transitional water body, depositing sediment in the lagoon which gets mixed with its waters, so that the final outflow to the Baltic is less coloured than that from the Vistula mouth (Figure 11). Figure 11b shows the SST image of the Vistula runoff distribution in May 2010, following one of the most extensive and disastrous spring floods in the last 100 years (Zajączkowski et al. 2010). The maximum river water discharge, measured at Tczew (35 km from the river mouth) on 25 May 2010, was 6838 m^3 s^{-1} (data from: www.armator.com.pl/stanwod/Wisla/Tczew/19). For comparison, the average water discharge near the Vistula mouth is 1080 m^3 s^{-1} (Pruszak et al. 2005).

The temperature gradient in Figure 11b shows that the wide distribution of the Vistula river plume is visible everywhere in the eastern Gulf of Gdask. It strongly influences the properties of the longshore current, which reaches Cape Taran and becomes incorporated into the N-Sambian eddy circulation, but here the strong SST anomaly ends, with only a small flux to the east remaining. Similar strong gradients and boundaries, or significant changes in form and size, of optically or SST-visible flows starting at the Gulf of Gdask and finishing in the N-Sambian eddy are observed in many other images (including Figures 11a,c,d). This indicates a complex and active vertical circulation within the N-Sambian eddy, an important subject to be further described.

In most cases one sees (e.g. Figures 9, 10, 11) the positive anomaly in the temperature field (the temperature within the N-Sambian eddy is higher than the temperature outside it), with an increase of this anomaly in
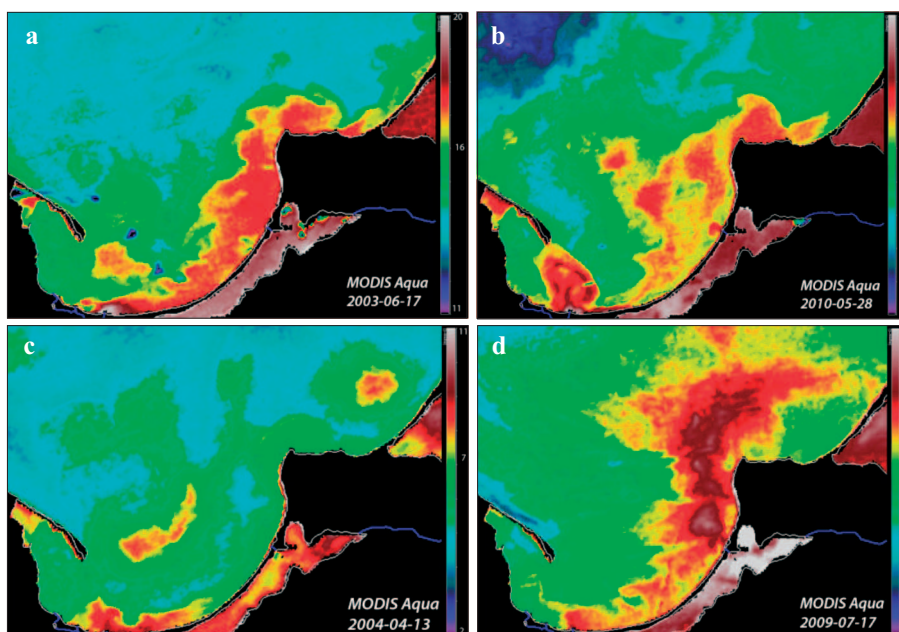
Figure 11. MODIS sea surface temperature (SST) maps, representing the distribution and transformation of the Vistula river plume in the Gulf of Gdańsk and the integration of these modified waters into the N-Sambian eddy

spring (Figure 10). In Figure 11d, which is the SST version of Figures 5a–b, SST is at a maximum on the west side of the eddy, but decreases towards the coast, and drops significantly eastwards, beyond the eddy zone. This again indicates the intensive and complex vertical dynamics of the eddy – downwelling blocks entrainment of deep and colder waters.

Only in four MODIS images from the 11-year archive was there evidence for an eddy structure to the west of Cape Taran, off the western coast of the Sambian Peninsula. Two examples of this eddy are presented in Figures 5c–d. Both were observed in summer after moderate N, NE or E winds (Table 1). The eddy had a spiral form (without any recognizable internal area like the N-Sambian eddy), diameters of 11 and 15 km for the two cases presentes on Figure 5, and a cyclonic circulation. It is probable that the general mechanism of eddy generation is the same as for the N-Sambian eddy, in this case driven by easterly winds causing the longshore flux to break away after having passed Cape Taran.

Much more frequently observed are narrow westward plumes from Cape Taran, and also from Cape Gvardeyskiy (Gurova 2009), formed from suspended sediments, and moving along the northern coast of the Sambian

Peninsula. The plumes moving away from Cape Taran reached 15–20 km in length, and varied in direction from westward to south-westward. Since the above-mentioned cyclonic eddies have been definitively identified only twice but plumes have been observed tens of times, we propose that the occurrence of the critical conditions for sub-mesoscale eddy formation is not a regular event when easterly winds are blowing.

3.2. Curonian Spit

Another area of interest is located seaward of the southern part of the Curonian Spit (near the village of Lesnoy), where sub-mesoscale eddies (hereafter referred to as the Lesnoy eddy) were measured several times using the CODAR technique. It was usually relatively small with a diameter of ca 6–10 km (Figures 3a–d), the maximum diameter being ca 14 km (Figures 3a, 6). Current speeds were different in every case (see Table 2) with maxima from 12 to 50 cm s^{-1}. We selected eight MODIS images with vortex-like structures in this area (see the examples on Figures 3e–f, 4a–b), but it should be noted that there is much more variance of appearance within this set than there is within the set of N-Sambian cases. Analysis of the preceding hydro-meteorological situation did not show any conformity with eddy appearance here, either in the CODAR or the MODIS data; the eddies were observed as occurring under completely different wind conditions, and with both SW and NE longshore current directions, but always with a cyclonic rotation of the eddy, as measured by CODAR. The few CODAR measurements that were obtainable during stormy weather with wind speeds higher than 10 m s^{-1} did not show any sub-mesoscale eddy here.

Even if the visible structures on the satellite images of this area (Figures 3e–f, Figures 4a–b) are not clearly identifiable as eddies, but rather resemble 'hooks' or open vortices, it should be noted that such forms can follow on from eddy circulation. Visualization of circulation structures in this area by satellite images is limited by the lack of coloured tracers – the mouths of large rivers are relatively distant, and very little river water reaches the Curonian Spit in any case, so only suspended sediments or heterogeneous algae concentrations can trace the sea currents in the area. The former depends very much on wind speeds, and the latter on the season and proximity to the coast. Additionally, the eddies' relatively small scale and probably the character of their circulation could be the reasons for their rare appearance on optical images. Consideration of the multiple CODAR measurements here during very different weather conditions leads to the suggestion that such eddies often arise near the southern part of the Curonian Spit and have a lifetime of at least one full day under stable wind conditions (as measured by CODAR on consecutive days). However, there

Table 2. Characteristics of eddies recorded by CODAR measurements

Date	Eddy place	R^1 [km]	Frequency distribution of current speed[2]
03.03.2006	Lesnoy	7	
04.04.2006	Lesnoy	5	
12.05.2006	Lesnoy	3.6	
24.05.2006	Lesnoy	4.2	
07.07.2006	Lesnoy	3	
26.08.2006	Central Curonian	15	
13.09.2006	N-Sambian	16.5	

[1] – radius,
[2] – x-axis – number of measurements (grid points), y-axis – current speed [cm s^{-1}], measured by CODAR.

is no information about the stability of such eddies over longer periods. Nevertheless, as this area is also one of the region's 'hot spots' in terms of combination of high recreational load, development potential and high rates of coastal erosion (Chubarenko et al. 2009), the Lesnoy eddy circulation and its influence on coastal processes should be further investigated in detail.

Several spiral eddies and vortex-like features have been identified on MODIS images in coastal waters near the central part of the Curonian Spit. They vary significantly in form, size, position, rotation direction and prevailing wind conditions (Figures 5e–i, Tables 1, 2), and this variance is also found on the relevant MODIS images. Only a few such structures

have been found in the 11-year MODIS archive, so we cannot regard them as frequent events affecting the coast, especially in cases like that shown on Figure 5e, where the eddy seems to be an element of the open-sea circulation.

4. Conclusions

This paper discusses the sub-mesoscale coastal eddies occurring in the coastal waters of the south-eastern Baltic, but does not give an explanation of the physical reasons for their appearance. While the N-Sambian eddy most probably seems to be formed as a wake eddy, the origins of the Lesnoy eddy and of the eddies near the Curonian Spit are still unclear. Different hypotheses generally related to the non-homogeneous structure of wind fields in space and time, or varied bottom topography, or complex interaction between upwelling/downwelling, combined with horizontal drift currents and local sea level gradients, need more evidence from measurements and numerical simulations, such as methodologies providing a different perspective to that supplied by the instantaneous radar-satellite photographs used here. Although the sources of information used in this paper are not methodologically homogeneous, and the radar and satellite observations have various resolutions and accuracy ranges, as well as various scales and times/conditions of exposure, some phenomenological conclusions can be drawn.

Sub-mesoscale eddies 10–20 km in diameter are regularly observed in the south-eastern Baltic under moderate and calm wind conditions. There are two particular locations off the northern shore of the Sambian Peninsula, where the occurrence of these eddies is probable: the N-Sambian eddy is located in the area adjacent to Cape Taran (between it and Cape Gvardeyskiy), while the Lesnoy eddy is located between the town of Zelenogradsk and the village of Lesnoy.

The N-Sambian eddy occurs when W and SW winds prevail, and has a maximum lifetime, as observed by daily remote sensing data, of up to 6 days. Many cases of its occurrence are clearly visible in satellite images. This eddy is always anticyclonic in circulation, appearing as a wake vortex after the longshore current around Cape Taran moves from south to north. Even the plume of Vistula river waters moving northwards along the Vistula Spit and partly modified by the entrainment of marine waters can sometimes be incorporated into the N-Sambian eddy circulation. The pattern of water property gradients and changes around the N-Sambian eddy indicates intensive and complex vertical components within its circulation. This is an important topic for further research.

The westward longshore flux driven by winds from the north-east quarter usually gives rise to plumes of suspended matter while passing the capes of the northern shore and Cape Taran on the Sambian Peninsula, but sometimes conditions become favourable for the generation of a small wake eddy (5–15 km in diameter) east of Cape Taran.

Although the Lesnoy eddy occurs frequently and is variable in its location, form and size, it is not strictly attributed to any form of the coastline off the base of the Curonian Spit, where the coastline changes direction from W-E to a SW-NE. The Lesnoy eddy does not form an obvious vortex signature on satellite images, and although vortex-like structures (mostly in form of a hook) in this area can be identified on MODIS images, even if this is relatively rare. The stability of the Lesnoy eddy in time and its influence on coastal processes should be further investigated.

The Lesnoy eddy as well as sub-mesoscale eddies near the central part of the Curonian Spit have different properties and dimensions in every case, and it is probable that the satellite imagery used here has only provided snapshots of the development of coastal eddies of different origins.

Acknowledgements

References

Aneer G., Löfgren S., 2007, *Algal bloom – some questions and answers*, County Admin. Board, Stockholm, 59 pp.

Babakov A. N., 2003, *Spatio-temporal structure of currents and sediment transport in the coastal zone of South-East Baltic (Sambian Peninsula and Curonian Spit)*, Ph. D. thesis, Kaliningrad, 273 pp., (in Russian).

Babakov A. N., Chubarenko B. V., Gorbatskiy V. V., Sivkov V. V., Gurova E. S., 2008, *Experience of surface currents remote measurements at the marine coast of Kaliningrad oblast*, Proceedings of the Kaliningrad Branch of the Russian Geographical Society, Vol. 7, Part 1 (CD-publication), Spec. issue, Kaliningrad, (in Russian).

Bassin C. J., Washburn L., Brzezinski M., McPhee-Shaw E., 2005, *Sub-mesoscale coastal eddies observed by high frequency radar: A new mechanism for delivering nutrients to kelp forests in South California Bight*, Geophys. Res. Lett., 32, L12604, http://dx.doi.org/10.1029/2005GL023017.

Boldyrev V. L., Lashenkov V. M., Ryabkova O. I., 1992, *Evolution of western coast of the Kaliningrad oblast under intensive anthropogenic influence*, [in:] *The evolution of the coasts under sea level rising*, Nauka Publ., Moscow, 212–225, (in Russian).

Brown O. B., Minnett P. J., 1999, *The MODIS infrared sea-surface temperature algorithm*, Algorithm technical basis document, NASA Goddard Space Flight Center, Greenbelt, Ver. 2.0,

Chubarenko B. V., Wang Y., Chubarenko I. P., Hutter K., 2000, *Barotropic wind-driven circulation pattern in a closed rectangular basin of variable depth influenced by a peninsula or an island*, Ann. Geophys., 18 (6), 706–727, http://dx.doi.org/10.1007/s00585-000-0706-6.

Emelyanov E. M., 1968, *Quantitative distribution of marine suspended matter near the coast of Sambian Peninsula – Curonian Spit (Baltic Sea)*, Oceanol. Invest., 18, 203–212, (in Russian).

Emelyanov E. M. (ed.), 2001, *Geology of the Gdańsk Basin, Baltic Sea*, Yantarny Skaz Publ., Kaliningrad, 494 pp.

Gorbatsky V., Gurova E., Babakov A., Chubarenko B., 2007, *Radar measurements of near-shore sea surface currents near the Curonian Spit (Kaliningrad Region)*, [in:] *Problems of the sea coastal zone management and sustainable development*, L. A. Zhindarev, R. D. Kos'yan & B. V. Divinsky (eds.), International Conference materials, Krasnodar, 65–67, (in Russian).

Gordon H. R., Wang M., 1994, *Retrieval of water-leaving radiance and aerosol optical thickness over the oceans with SeaWiFS: A preliminary algorithm*, Appl. Optics, 33 (3), 443–452, http://dx.doi.org/10.1364/AO.33.000443.

Gurova E., 2009, *Methodological aspects of the use of MODIS satellite images for assessment of suspended matter distribution in coastal waters of South-Eastern Baltic, artificial beaches, artificial islands and other structures in the coastal and offshore areas*, Proc. Int. Conf. 'Construction of the artificial lands in the coastal and offshore areas', Novosibirsk, 2009, A. Sh. Khabidov (ed.), 130–140, (in Russian).

Gurova E., Chubarenko B., Sivkov V., 2008, *Transboundary coastal waters of the Kaliningrad oblast*, [in:] *Transboundary waters and basins in the South-East Baltic*, B. Chubarenko (ed.), Terra Baltica, Kaliningrad, 37–57.

Gurova E., Ivanov A. Y., 2011, *Appearance of sea surface signatures and current features in the south-east Baltic Sea on the MODIS and SAR images*, Issled. Zemli Kosm., 4, 41–54, (in Russian).

Harlan J. A., Swearer S. E., Leben R. R., Fox C. A., 2002, *Surface circulation in a Caribbean island wake*, Cont. Shelf Res., 22 (3), 417–434, http://dx.doi.org/10.1016/S0278-4343(01)00073-5.

IOCCG, 2000, *Remote sensing of ocean colour in coastal, and other optically-complex, waters*, S. Sathyendranath (ed.), Rep. Int. Ocean-Colour Coord. Group, No. 3, IOCCG, Dartmouth, 140 pp.

Ivanov A. Y., 2010, *On extraction of marine environmental parameters from spaceborne SAR data*, Issled. Zemli Kosm., 3, 77–92.

Ivanov A. Y., Ginzburg A. I., 2002, *Oceanic eddies in synthetic aperture radar images*, Proc. Indian Acad. Sci. (Earth Planet. Sci.), 111 (3), 281–295.

Johannessen J. A., Espedal H., Johannessen O. M., 1994, *SAR Ocean Feature Catalogue*, ESA Publ. Divis. ESTEC, ESA SP-1174, Noordwijk, 106 pp.

Karabashev G. S., Evdoshenko M. A., Sheberstov S. V., 2005, *Analysis of the manifestation of mesoscale water exchange in satellite images of the sea surface*, Oceanology, 45 (2), 195–205.

Kowalczuk P., 1999, *Seasonal variability of yellow substance absorption in the surface layer of the Baltic Sea*, J. Geophys. Res., 104 (C12), 30 047–30 058, http://dx.doi.org/10.1029/1999JC900198.

Kowalczuk P., Darecki M., Zabłocka M., Górecka I., 2010, *Validation of empirical and semi-analytical remote sensing algorithms for estimating absorption by Coloured Dissolved Organic Matter in the Baltic Sea from SeaWiFS and MODIS imagery*, Oceanologia, 52 (2), 171–196, http://dx.doi.org/10.5697/oc.52-2.171.

Kowalczuk P., Olszewski J., Darecki M., Kaczmarek S., 2005, *Empirical relationships between coloured dissolved organic matter (CDOM) absorption and apparent optical properties in Baltic Sea waters*, Int. J. Remote Sens., 26 (2), 345–370, http://dx.doi.org/10.1080/01431160410001720270.

Lee Z. P., Darecki M., Carder K. L., Curtiss O. D., Stramski D., Rhea W. J., 2005, *Diffuse attenuation coefficient of downwelling irradiance: an evaluation of remote sensing methods*, J. Geophys. Res., 110, C02017, 148–227, http://dx.doi.org/10.1029/2004JC002573.

Pruszak Z., van Ninh P., Szmytkiewicz M., Manh Hung N., Ostrowski R., 2005, *Hydrology and morphology of two river mouth regions (temperate Vistula Delta and subtropical Red River Delta)*, Oceanologia, 47 (3), 365–385.

Ruddick K. G., Ovidio F., Rijkeboer M., 2000, *Atmospheric correction of SeaWiFS imagery for turbid coastal and inland waters*, Appl. Optics, 39 (6), 897–912, http://dx.doi.org/10.1364/AO.39.000897.

Rudolph C., Lehmann A., 2006, *A model-measurements comparison of atmospheric forcing and surface fluxes of the Baltic Sea*, Oceanologia, 48 (3), 333–360.

Ryabkova O. I., 1987, *Coastal dynamics of the Sambian Peninsula and Curonian Spit owing to coastal defense problems*, Ph. D. thesis, Moscow State Univ., 306 pp., (in Russian).

Woźniak B., Dera J., 2007, *Light absorption in sea water*, Springer, Dordrecht, 456 pp.

Woźniak B., Krężel A., Darecki M., Woźniak S. B., Majchrowski R., Ostrowska M., Kozłowski Ł., Ficek D., Olszewski J., Dera J., 2008, *Algorithm for the remote sensing of the Baltic ecosystem (DESAMBEM). Part 1: Mathematical apparatus*, Oceanologia, 50 (4), 451–508.

Zajączkowski M., Darecki M., Szczuciński W., 2010, *Report on the development of the Vistula river plume in the coastal waters of the Gulf of Gdańsk during the May 2010 flood*, Oceanologia, 52 (2), 311–317, http://dx.doi.org/10.5697/oc. 52-2.311.

Zatsepin A. G., Baranov V. I., Kondrashov A. A., Korzh A. O., Kremenetskiy V. V., Ostrovskii A. G., Soloviev D. M., 2011, *Submesoscale eddies over the Caucasus Black Sea shelf and the mechanisms of their generation*, Oceanology, 51 (4), 554–567, http://dx.doi.org/10.1134/S0001437011040205.

Zhindarev L. A., Khabidov A. Sh., Trizno A. K., 1998, *Coastal dynamics of seas and inland waterbodies*, Nauka, Siberian Enterprise RAS, Novosibirsk, 271 pp., (in Russian).